

Arbitrary Power-Division Branch-Line Hybrids for High-Performance, Wideband, and Selective HarmonicSuppressions From $2f_0$

Hee-Ran Ahn¹, Senior Member, IEEE, and Manos M. Tentzeris², Fellow, IEEE

Abstract—A branch-line hybrid (BH) topology is suggested, consisting of four equal lengths of transmission-line sections (TLs) with two different characteristic impedances and four identical L -sections with each a TL and an open stub. The topology can provide three distinct properties; lower characteristic impedances of TLs, longer electrical paths for the scattering parameters, and additional transmission zeros, enabling high performance of harmonic suppressions from $2f_0$, where f_0 is a design frequency, wideband and selective harmonic suppressions. A compact equivalent circuit of a TL is suggested for harmonic suppression BH which can be applied for all possible power-division ratios. As a proof-of-concept demonstration, two prototypes for the power-division ratios of 0 and 6 dB are tested and measured. The measured frequency responses are in a good agreement with the predicted ones, given fabrication errors.

Index Terms—Arbitrary power-division ratios, branch-line couplers, branch-line hybrids (BHs), harmonic suppression BHs (HSBHs), quadrature couplers, selective and wideband harmonic suppressions.

I. INTRODUCTION

BRANCH-LINE hybrids (BHs) or quadrature couplers [1]–[15] are important key components for RF/MW wireless communication systems, providing equal/arbitrary power-division ratios with 90° phase differences between two outputs. The conventional BH consists of four 90° transmission-line sections (TLs), thus featuring higher order harmonics which can interfere with other equipments. To filter out such unwanted harmonics, several attempts have been tried but the previous methods [3]–[15] have restrictions on desired harmonic suppressions from $2f_0$, where f_0 is a design frequency, wideband and selective harmonic suppressions.

A uniform 90° TL can produce $(2n - 1)f_0$ harmonics, where n is integer, but cannot have any function to produce transmission zeros (TZs) with which harmonics can be suppressed. So, for the harmonic suppressions, equivalent circuits of the TLs are required such as the impedance varying 90° TLs [3], a parallel connection of a TL and a capacitor [4],

Manuscript received May 21, 2018; revised September 14, 2018, October 14, 2018, November 3, 2018 and November 23, 2018; accepted November 29, 2018. Date of publication February 6, 2019; date of current version March 5, 2019. This work was supported in part by the NSF and in part by the EFRI. (Corresponding author: Hee-Ran Ahn.)

The authors are with the School of Electrical and Computer Engineering, Georgia Institute of Technology, Atlanta, GA 30332 USA (e-mail: hranahn@gmail.com; etentze@ece.gatech.edu).

Color versions of one or more of the figures in this paper are available online at <http://ieeexplore.ieee.org>.

Digital Object Identifier 10.1109/TMTT.2019.2892444

Π - [5], [7], [9], [14] and T -types [8], [10], [14], L_T -type [16, Fig. 5(c) with $N = 1$] in [14], using coupled TLs [6], [11], [15], artificial equivalent circuit [12], or two parallel TLs [13]. However, they have restrictions on $2f_0$ suppressions [3]–[6], [8], [10]–[12] which are fundamentally important for the wireless communication systems, because the signals with $2f_0$ cannot be ignored from adjacent active components including diodes. The harmonics treated in all the works [3]–[15] cannot be suppressed selectively, and high performance with wideband harmonic suppressions do not seem to be possible, either. All the equivalent circuits [3]–[15] for the harmonic suppressions cannot be applied for all possible power-division ratios of BHs. For example, the L_T -types used in [14] and [16] are not good candidates for the equal power divisions, because the L_T -type is an alternative high-impedance TL [16]. The Π - or T -type [17] is not suitable for high power-division ratios.

To alleviate the conventional problems, a BH topology is, in this paper, suggested, consisting of two sets of TLs and four identical L -sections with each a TL and an open stub. This suggested topology can provide as low characteristic impedances of the TLs as possible, the longer electrical paths for the scattering parameters and four additional open stubs for the different TZs, being able to provide $2f_0$ signal suppression, high-performance harmonic suppression (more than 30 dB suppression), wideband and selective harmonic suppressions.

For harmonic suppression BHs (HSBHs), a compact equivalent circuit of a TL is suggested, consisting of two identical TLs, two identical inductances and two T-types which can be applied for any power-division ratio, because the suggested equivalent circuit can alleviate the fabrication difficulties of high impedance TLs, when the power-division ratios are high. As the proof-of-concept demonstration, two prototypes for the power-division ratios of 0 dB and 6 dB are designed, fabricated and measured at the design frequency of 1 GHz. The simulated (measured) results demonstrate more than 30-dB harmonic suppressions, wideband ($2f_0 - 4f_0$) and selective harmonic suppressions whose performance can be considered to be excellent compared to [3]–[15].

II. SUGGESTED BH

The suggested BH terminated in equal impedances of Z_0 is depicted in Fig. 1, consisting of four equal lengths (Θ) of TLs and four L -sections. Two TLs with the characteristic

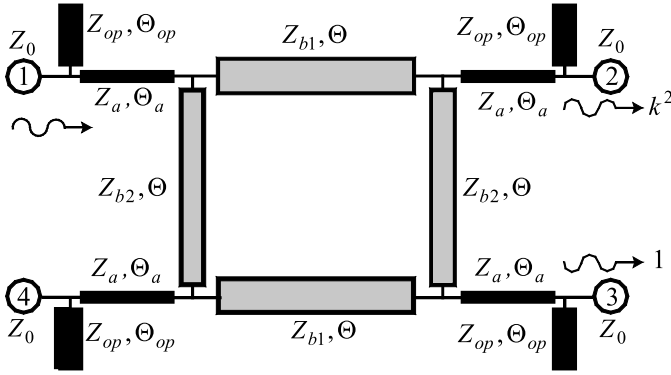


Fig. 1. Suggested BH.

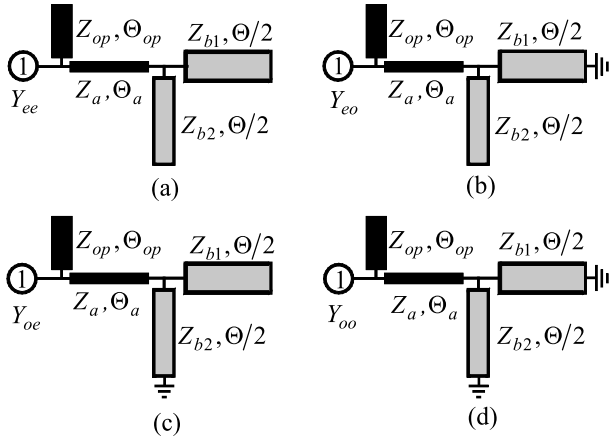


Fig. 2. Even- and odd-mode equivalent circuits. (a) Even-even (ee) equivalent circuit. (b) Even-odd (eo) equivalent circuit. (c) Odd-even (oe) equivalent circuit. (d) Odd-odd (oo) equivalent circuit.

impedance of Z_{b1} are identical, located horizontally in parallel, and the other two with the characteristic impedance of Z_{b2} are also identical, located vertically in parallel. Each L -section is composed of one TL with Z_a and Θ_a and one open stub with the characteristic impedance of Z_{op} and the electrical length of Θ_{op} . The power excited at port ① is divided into ports ② and ③ with the power-division ratio of k^2 as indicated and isolated at port ④ where $k^2 \geq 1$ is assumed.

A. Design Formulas

The suggested BH in Fig. 1 has two-fold symmetry axes, leading to four even-even (ee), even-odd (eo), odd-even (oe), and odd-odd (oo) equivalent circuits being possible as depicted in Fig. 2. The input admittances of Y_{ee} , Y_{eo} , Y_{oe} , and Y_{oo} , where the subscripts of ee, eo, oe and oo are related with the equivalent circuits in Fig. 2, are

$$Y_{ee} = jS_u + Y_a \frac{Y_{eeL} + jY_a \tan \Theta_a}{Y_a + jY_{eeL} \tan \Theta_a} \quad (1a)$$

$$Y_{eo} = jS_u + Y_a \frac{Y_{eoL} + jY_a \tan \Theta_a}{Y_a + jY_{eoL} \tan \Theta_a} \quad (1b)$$

$$Y_{oe} = jS_u + Y_a \frac{Y_{oeL} + jY_a \tan \Theta_a}{Y_a + jY_{oeL} \tan \Theta_a} \quad (1c)$$

$$Y_{oo} = jS_u + Y_a \frac{Y_{ooL} + jY_a \tan \Theta_a}{Y_a + jY_{ooL} \tan \Theta_a} \quad (1d)$$

where $S_u = Y_{op} \tan \Theta_{op}$, $Y_a = Z_a^{-1}$, and when $\Theta = 90^\circ$, the values of Y_{eeL} , Y_{eoL} , Y_{oeL} and Y_{ooL} are

$$Y_{eeL} = j(Y_{b1} + Y_{b2}) \quad Y_{eoL} = j(-Y_{b1} + Y_{b2}) \quad (1e)$$

$$Y_{oeL} = j(Y_{b1} - Y_{b2}) \quad Y_{ooL} = -j(Y_{b1} + Y_{b2}) \quad (1f)$$

with $Y_{b1} = Z_{b1}^{-1}$ and $Y_{b2} = Z_{b2}^{-1}$.

The reflection coefficients related with the input impedances are

$$\Gamma_{ee} = -\frac{Y_{ee} - Y_0}{Y_{ee} + Y_0} \quad \Gamma_{eo} = -\frac{Y_{eo} - Y_0}{Y_{eo} + Y_0} \quad (2a)$$

$$\Gamma_{oe} = -\frac{Y_{oe} - Y_0}{Y_{oe} + Y_0} \quad \Gamma_{oo} = -\frac{Y_{oo} - Y_0}{Y_{oo} + Y_0} \quad (2b)$$

where $Y_0 = Z_0^{-1}$.

Using the reflection coefficients in (2), all port scattering parameters [18] can be obtained as

$$S_{11} = \frac{(\Gamma_{ee} + \Gamma_{eo}) + (\Gamma_{oe} + \Gamma_{oo})}{4} \quad (3a)$$

$$S_{21} = \frac{(\Gamma_{ee} - \Gamma_{eo}) + (\Gamma_{oe} - \Gamma_{oo})}{4} \quad (3b)$$

$$S_{31} = \frac{(\Gamma_{ee} - \Gamma_{eo}) - (\Gamma_{oe} - \Gamma_{oo})}{4} \quad (3c)$$

$$S_{41} = \frac{(\Gamma_{ee} + \Gamma_{eo}) - (\Gamma_{oe} + \Gamma_{oo})}{4} \quad (3d)$$

For the perfect matching at port ① and perfect isolation at port ④, or, $S_{11} = S_{41} = 0$ in (3), the following relations hold:

$$\Gamma_{ee} + \Gamma_{eo} = 0 \quad (4a)$$

$$\Gamma_{oe} + \Gamma_{oo} = 0. \quad (4b)$$

Substituting the reflection coefficients in (2) into (4) gives

$$Y_{ee}Y_{eo} = Y_{oe}Y_{oo} = Y_0^2. \quad (5)$$

To satisfy the power-division ratio of k^2 and the 90° phase difference, the relation between the two scattering parameters of S_{21} and S_{31} should be

$$S_{21} = jkS_{31}. \quad (6)$$

Substituting (2) and (3) into (6) results in

$$(Y_{eo}Y_{oo} - Y_0^2) = jk(Y_{eo} - Y_{oo})Y_0. \quad (7)$$

Input impedances in (1) being substituted into (5) and (7), (8) can be derived as

$$A + B = Y_0^2 \{ Y_a^2 - (Y_{b1}^2 - Y_{b2}^2) \tan^2 \Theta_a \} \quad (8a)$$

$$C = Y_0^2 \tan \Theta_a \quad (8b)$$

$$\begin{aligned} -A + B + 2Y_a Y_{b1} C + D \\ = -2kY_0 Y_a^2 Y_{b2} \sec^2 \Theta_a \end{aligned} \quad (8c)$$

where

$$A = (Y_{b1}^2 - Y_{b2}^2)(Y_a - S_u \tan \Theta_a)^2 \quad (8d)$$

$$B = -Y_a^2 (S_u + Y_a \tan \Theta_a)^2 \quad (8e)$$

$$C = (S_u + Y_a \tan \Theta_a)(Y_a - S_u \tan \Theta_a) \quad (8f)$$

$$D = -Y_0^2 \{ Y_a^2 + 2Y_{b1} Y_a \tan \Theta_a + (Y_{b1}^2 - Y_{b2}^2) \tan^2 \Theta_a \}. \quad (8g)$$

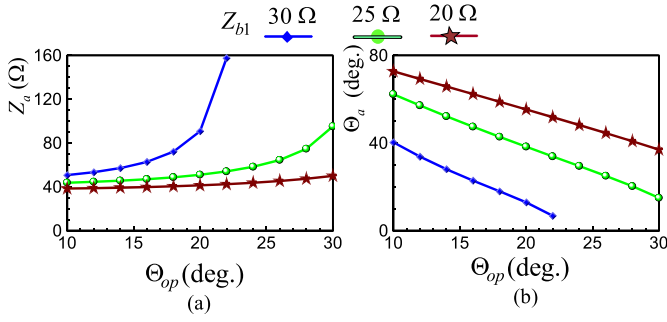


Fig. 3. Calculated values of Z_a and Θ_a for $k = 1$ and $Z_{op} = 50 \Omega$. (a) Z_a . (b) Θ_a .

Since the purpose of the suggested BH is to get the characteristic impedances lower than those of the conventional BHs, the values of Z_{b1} should be

$$Z_{b1} < Z_0 \sqrt{k^2 / (k^2 + 1)}. \quad (9)$$

The unknown variables are 5 (susceptance $S_u = Y_{op} \tan \Theta_{op}$, Y_a , Θ_a , Z_{b1} , and Z_{b2}) in Fig. 1 with $\Theta = 90^\circ$, and the available conditions in (8) are three. Therefore, two parameters for Z_{b1} and S_u should be predetermined arbitrarily. The values for Z_{b1} can be determined freely based on (9), while those for S_u should be determined to have proper values of Y_a and Θ_a . Three design formulas for Z_{b2} , $Y_a = Z_a^{-1}$, and Θ_a can be derived in the following equations:

$$Z_{b2} = Z_{b1} \sqrt{1 + k^2} \quad (10a)$$

$$Z_a = \sqrt{\frac{T_r(R_G^2 + X_G^2) - R_G T_r^2}{R_G - T_r}} \quad (10b)$$

$$\tan \Theta_a = \frac{Z_a X_G}{T_r R_G - Z_a^2} \quad (10c)$$

where Z_a is of real values and

$$\left(\frac{1}{Z_0} + j S_u \right)^{-1} = R_G + j X_G \quad (10d)$$

$$T_r = Z_{b1} \sqrt{\frac{1 + k^2}{k^2}}. \quad (10e)$$

Based on the design formulas in (10), the values of Z_a and Θ_a were, for $k = 1$ and $Z_{op} = 50 \Omega$, calculated by varying Θ_{op} and $Z_{b1} = 20, 25,$ and 30Ω and plotted in Fig. 3(a) and (b), respectively. When $\Theta_{op} = 23^\circ$ in Fig. 3(a), the real values for Z_a and Θ_a do not exist for $Z_{b1} = 30 \Omega$, but those for $Z_{b1} = 25$ and 20Ω are possible even when $\Theta_{op} = 30^\circ$. The characteristic impedances Z_a are proportional to Θ_{op} , while the electrical lengths of Θ_a are inversely proportional to Θ_{op} . That is, the characteristic impedances of Z_a are inversely proportional to the electrical lengths of Θ_a , and higher value of Z_{b1} gives higher value of Z_a and shorter length of Θ_a .

B. Frequency Responses of Suggested BHs for $k = 2$

The design parameters for $k = 2$, or, power-division ratio of 6 dB can be calculated based on the design formulas (10). The values of Z_{b1} can be chosen as 35 and 30Ω arbitrarily

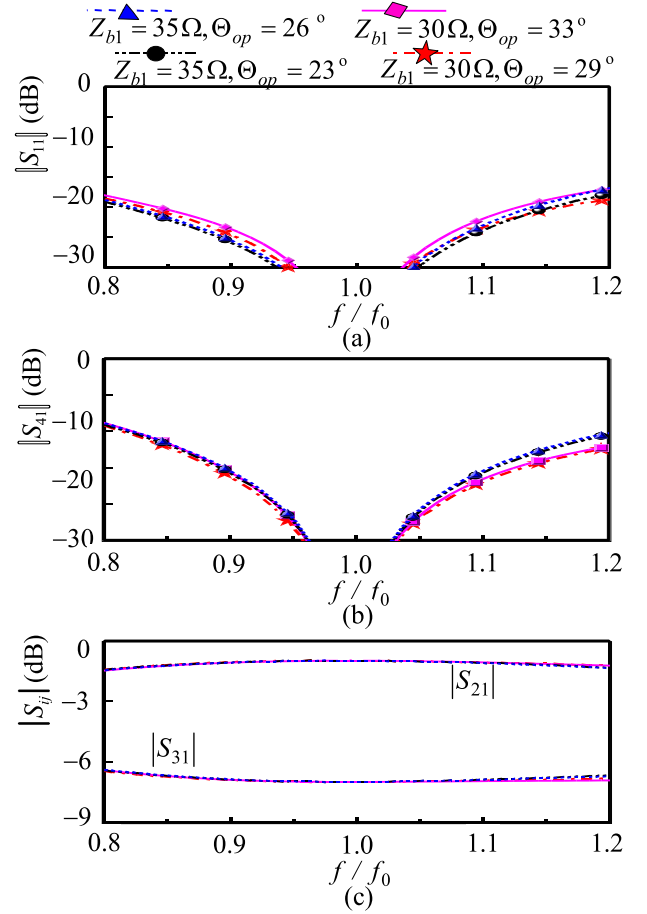


Fig. 4. Frequency responses of BHs for $k = 2$. (a) Matchings at port ① $|S_{11}|$. (b) Isolations at port ④ $|S_{41}|$. (c) Power divisions of $|S_{21}|$ and $|S_{31}|$.

based on (9), leading to $Z_{b2} = 78.26$ and 67.08Ω in (10a), respectively. For the two cases with $(Z_{b1}, Z_{b2}) = (35 \Omega, 78.26 \Omega)$ and $(30 \Omega, 67.08 \Omega)$, fixing $Z_0 = Z_{op} = 50 \Omega$, the values of Z_a and Θ_a are calculated as listed in Table I. Two BHs with $(Z_{b1}, \Theta_{op}) = (35 \Omega, 26^\circ)$, $(35 \Omega, 23^\circ)$ and the other two with $(Z_{b1}, \Theta_{op}) = (30 \Omega, 33^\circ)$, $(30 \Omega, 29^\circ)$ in Table I were simulated using a circuit simulator ADS, and the frequency responses are plotted in Fig. 4 where f and f_0 are operating and design frequencies, respectively. The matching responses at port ① and the isolations at port ④ are plotted in Fig. 4(a) and (b), respectively, while the power divisions in Fig. 4(c). As can be seen, the near-perfect matchings at port ① and isolations at port ④ can be achieved at f_0 , while the near-perfect power divisions with $|S_{21}| = -0.97$ dB and $|S_{31}| = -6.97$ dB can be achieved at f_0 , as well.

III. HARMONIC SUPPRESSION BHs

To allocate the wanted TZs for the harmonic suppressions selectively, equivalent circuits for the TLs with Z_{b1} and Z_{b2} are required. As listed in Table I for $k = 2$, the characteristic impedances of the TLs for Z_{b1} are sufficiently low compared to the conventional BHs. On the other hand, those for Z_{b2} are lower than the conventional BHs but higher than those for Z_{b1} , leading to T-types or Π -types being extremely difficult due

TABLE I
DESIGN PARAMETERS OF SUGGESTED BHs
FOR $k = 2$ AND $Z_0 = Z_{op} = 50 \Omega$

| $Z_{b1}(\Omega)$ | $Z_{b2}(\Omega)$ | $\Theta_{op}(\circ)$ | $Z_a(\Omega)$ | $\Theta_a(\circ)$ |
|------------------|------------------|----------------------|---------------|-------------------|
| 35 | 78.26 | 26 | 116.75 | 10.81 |
| | | 25 | 94.92 | 13.80 |
| | | 23 | 74.63 | 18.94 |
| | | 21 | 64.56 | 23.68 |
| 30 | 67.08 | 33 | 109.22 | 13.06 |
| | | 31 | 79.66 | 18.98 |
| | | 29 | 66.98 | 23.91 |
| | | 27 | 59.67 | 28.43 |

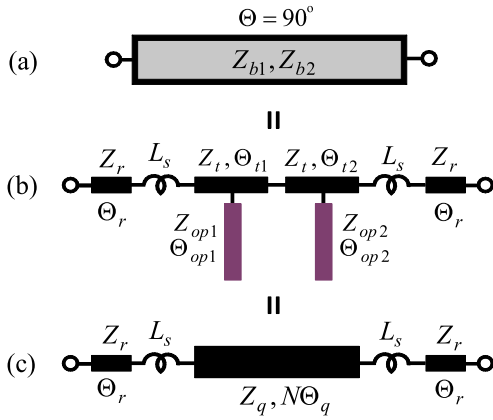


Fig. 5. Equivalent circuits. (a) 90° TL with Z_{b1} or Z_{b2} . (b) $ML_{s2}T$ -type. (c) Compact equivalent circuit of $ML_{s2}T$ -type under the condition of $\Theta_{t1} = \Theta_{t2}$ or $\Theta_{t2} = 0^\circ$.

to unfeasible characteristic impedances of TLs [17] when the power-division ratios are high. Therefore, any novel compact equivalent circuit of a TL is required which can be applied for any value of k .

A. Equivalent Circuit of $ML_{s2}T$ -Type

A 90° TL with Z_{b1} or Z_{b2} and its compact equivalent circuit named $ML_{s2}T$ -type are depicted in Fig. 5(a) and (b), respectively, which consists of two identical TLs with Z_r and Θ_r , two identical inductances L_s and two T-types with the same Z_t and two electrical lengths of Θ_{t1} and Θ_{t2} , and two different open stubs with (Z_{op1}, Θ_{op1}) and (Z_{op2}, Θ_{op2}) . The T-types, each open stub of which is located at the center of each TL, have the same susceptances, namely $Y_{op1} \tan \Theta_{op1} = Y_{op2} \tan \Theta_{op2}$, where $Y_{op1} = Z_{op1}^{-1}$ and $Y_{op2} = Z_{op2}^{-1}$. The role of the identical inductances is to lower the characteristic impedances of Z_t , and the role of the TLs with Z_r and Θ_r is to solder the chip inductors successfully. So, if there is no use of L_s , the two identical TLs with Z_r and Θ_r are not necessary, either.

If the circuit with two T-types is symmetric with $\Theta_{t1} = \Theta_{t2}$ or $\Theta_{t2} = 0$ in Fig. 5(b), the two T-types can be equivalent to a uniform TL with the assumed characteristic

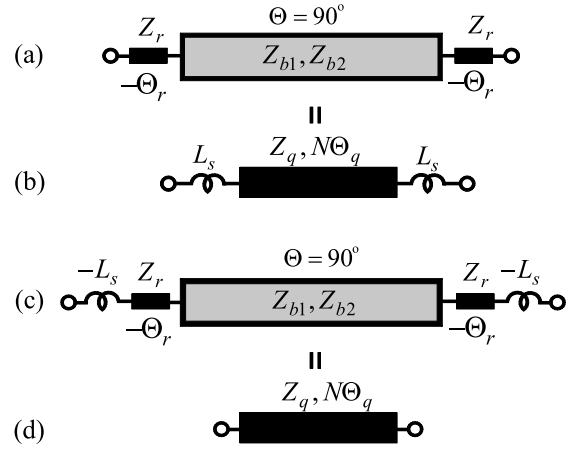


Fig. 6. Easy derivation process. (a) and (b) Connecting two identical TLs with Z_r and $-\Theta_r$ to both sides of the circuits in Fig. 5(a) and (c). (c) and (d) Connecting two identical $-L_s$ s to both sides of the circuits in (a) and (b).

impedance of Z_q and electrical length of $N\Theta_q$ as shown in Fig. 5(c), where $N = 1$ or 2 . For $N = 1$, one T-type is possible with $\Theta_{t1} = \Theta_t$ and $\Theta_{t2} = 0$, and if $N = 2$ is applied, two T-types are possible with $\Theta_{t1} = \Theta_{t1} = \Theta_t$. The inductance values of L_s are generally limited and necessary only for high power-division ratios. Thus the values of Z_r , Θ_r and L_s should be predetermined arbitrarily depending on the fabrication situation such as the values of Z_{b2} , substrates, chip inductor values and sizes.

Therefore, the targeting design values should be the two T-types in Fig. 5(b) and the TL with Z_q and $N\Theta_q$ in Fig. 5(c) should be derived first. To make derivation process easier, two identical TLs with Z_r and $-\Theta_r$ are connected to both sides of each circuit in Fig. 5(a) and (c), resulting in two circuits in Fig. 6(a) and (b), respectively, because two series TLs with $-\Theta_r$ and Θ_r are the same as no TL connected. Similarly, connecting two identical $-L_s$ to both sides of the two circuits in Fig. 6(a) and (b) gives those in Fig. 6(c) and (d), respectively, because the series connection of $-L_s$ and L_s is the same as no inductance connected.

The even- and odd-mode impedances in Fig. 6(c) are

$$Z_{ev1} = -j\omega L_s - jZ_r \frac{Z_{bi} + Z_r \tan \Theta_r}{Z_r - Z_{bi} \tan \Theta_r} \quad (11a)$$

$$Z_{od1} = -j\omega L_s + jZ_r \frac{Z_{bi} - Z_r \tan \Theta_r}{Z_r + Z_{bi} \tan \Theta_r} \quad (11b)$$

where Z_{bi} is Z_{b1} or Z_{b2} . Those in Fig. 6(d) are

$$Z_{ev2} = -jZ_q \cot \frac{N\Theta_q}{2} \quad (12a)$$

$$Z_{od2} = jZ_q \tan \frac{N\Theta_q}{2}. \quad (12b)$$

Equating both impedances $Z_{ev1} = Z_{ev2}$ and $Z_{od1} = Z_{od2}$ in (11) and (12) and predetermining N , L_s , Z_r , and Θ_r arbitrarily depending on the values of Z_{b1} and Z_{b2} and fabrication situation, the design formulas for Z_q and $N\Theta_q$ can be

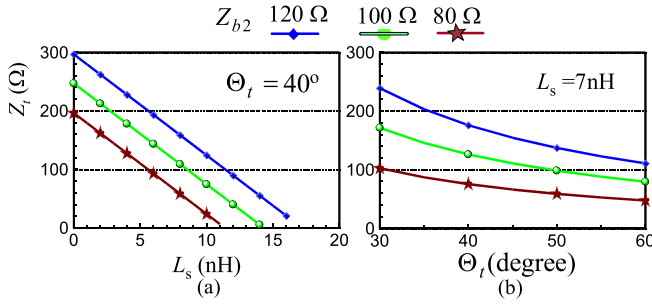


Fig. 7. Calculation values of Z_t fixing at $Z_r = 110 \Omega$ and $\Theta_r = 3^\circ$. (a) Z_t by varying L_s . (b) Z_t by varying Θ_t .

derived as

$$Z_q = \sqrt{\frac{(Z_r \xi_+ - \omega L_s Z_{bi} \tan \Theta_r)(Z_r \xi_- - \omega L_s Z_{bi} \tan \Theta_r)}{Z_r^2 - (Z_{bi} \tan \Theta_r)^2}} \quad (13a)$$

$$\tan \frac{N \Theta_q}{2} = \sqrt{\frac{(Z_r - Z_{bi} \tan \Theta_r)}{(Z_r + Z_{bi} \tan \Theta_r)} \left(\frac{Z_r \xi_- - \omega L_s Z_{bi} \tan \Theta_r}{Z_r \xi_+ - \omega L_s Z_{bi} \tan \Theta_r} \right)} \quad (13b)$$

where Z_q and Θ_q are of real values and

$$\begin{aligned} \xi_+ &= (Z_{bi} + Z_r \tan \Theta_r + \omega L_s) \\ \xi_- &= (Z_{bi} - Z_r \tan \Theta_r - \omega L_s). \end{aligned}$$

To design suitable values for Z_t of one or two T -types from the two values of Z_q and Θ_q in (13), the electrical lengths of Θ_t should be adjusted [17, eq. (13)] using the following formulas:

$$Z_t = Z_q \frac{\tan \frac{\Theta_q}{2}}{\tan \frac{\Theta_t}{2}} \quad (14a)$$

$$\tan \Theta_{\text{opj}} = \frac{2Z_{\text{opj}}}{Z_t} \frac{Z_t - Z_q \cot \frac{\Theta_q}{2} \tan \frac{\Theta_t}{2}}{Z_t \tan \frac{\Theta_t}{2} + Z_q \cot \frac{\Theta_q}{2}} \quad (14b)$$

where the subscript of j is 1 and 2 and values of Θ_{opj} in (14b) can be determined depending on the desired TZ frequency f_{zj} based on the following formula:

$$\Theta_{\text{opj}} = \frac{\pi}{2f_{zj}}. \quad (15)$$

If the values of Z_{b1} or Z_{b2} are low less than 45Ω , $N = 2$ with $L_s = \Theta_r = 0$ is an alternative choice. Otherwise $N = 1$ with $L_s \neq \Theta_r \neq 0$ is recommended. In this case for $N = 1$, the characteristic impedances of Z_t were, fixing at $Z_r = 110 \Omega$ and $\Theta_r = 3^\circ$, calculated by varying L_s and Θ_t and plotted in Fig. 7 where $f_0 = 1 \text{ GHz}$. Since $k \geq 1$ is assumed, Z_{b2} is always greater than Z_{b1} and the characteristic impedances of $Z_{b2} = 80, 100, \text{ and } 120 \Omega$ in Fig. 7 were selected randomly. The calculated values of Z_t in Fig. 7 are inversely proportional to the inductance values L_s in Fig. 7(a) and electrical lengths Θ_t in Fig. 7(b). Higher values of Z_{b2} give higher values of Z_t . Referring to the relations in Fig. 7, the $ML_{s2}T$ -types can be achieved in any case by choosing appropriate values of L_s and Θ_t , even for high values of Z_{b2} or k .

B. Design Guidelines

The design guidelines for the HSBHs are as follows.

- 1) For a given power-division ratio k , choose the value of $Z_{b1} < Z_0(k^2/(k^2 + 1))^{1/2}$ in (9) arbitrarily.
- 2) The value of Z_{b2} can be calculated using (10a).
- 3) Based on arbitrarily chosen value of S_{u1} , the L -section with Z_a and Θ_a can be calculated using (10b) and (10c). Now the BHs are ready for HSBHs by replacing of the TLs with the $ML_{s2}T$ -types.
- 4) Depending on the values of Z_{b1} and Z_{b2} , the compact equivalent circuit of $ML_{s2}T$ -type for the HSBHs can be designed differently.
- 5) For any value of Z_{b1} and the values of $Z_{b2} \leq 45 \Omega$, $N = 2$ and $L_s = \Theta_r = 0$ can be applied for the $ML_{s2}T$ -type, leading to the modified T-types with $N = 2$ [17].
- 6) For the high values of Z_{b2} , the inductances of L_s are required to alleviate a fabrication difficulty, leading to $N = 1$ and $L_s \neq \Theta_r \neq 0$.
- 7) Since the chip inductance values are limited by the manufacturers, select available inductance values, referring to the plots in Fig. 7.
- 8) The TLs with Z_r and Θ_r are required to solder the chip inductors successfully and therefore should be determined depending on chip inductor sizes, substrates and the design frequency.
- 9) For high values of Z_{b2} , with the predetermined values of $N = 1$, L_s , Z_r , and Θ_r , the highest feasible value of Z_t can be calculated by adjusting Θ_t , referring to Fig. 7.
- 10) Depending on the desired TZs, the values of Θ_{opj} of the L -sections and Θ_{opj} of the $ML_{s2}T$ -type can be designed based on (15). If the number of TZs is not sufficient for the S_{21} -path, any additional TZ can be obtained by designing the open stubs of the L -sections differently.
- 11) Note that the best harmonic suppression for S_{21} can be achieved with the highest feasible characteristic impedances of TLs.

Even if one open stub can provide one TZ, it is not guaranteed that the signals between two TZs can be sufficiently suppressed. For example, even though the TZs at $2f_0$, $3f_0$, and $4f_0$ can be achieved successfully, the signals cannot be suppressed between $2f_0$ and $4f_0$ by more than 30 dB in the previous designs [3]–[13]. However, the suggested BH in Fig. 1 and the $ML_{s2}T$ -type can provide such wideband harmonic suppressions, which is the unique property of this work.

Because the concerned scattering parameters are S_{21} and S_{31} , the power flow paths for S_{21} and S_{31} are necessary to know for the harmonic suppressions. When the power is excited at port ① in Fig. 1, the power flow path for S_{21} [1] is the L -section at port ① \rightarrow the TL with Z_{b1} \rightarrow another L -section \rightarrow port ②, while that for S_{31} is the L -section at port ① \rightarrow the TL with Z_{b1} \rightarrow the TL with Z_{b2} \rightarrow another L -section \rightarrow port ③. That is, some parts for S_{21} are overlapped for the S_{31} path. Therefore, how to allocate the wanted TZs through the S_{21} -path is important. For example, if the TZs at $2f_0$, $3f_0$ and $4f_0$ are desired, three open stubs can be designed

TABLE II
DESIGN AND FABRICATION PARAMETERS FOR $k = 1$

| |
|---|
| $Z_{b1} = 28.28 \Omega$, $Z_{b2} = 40 \Omega$ with $\Theta_r = L_s = 0$ and $N = 2$ |
| $Z_a = 108.6 \Omega$, $\Theta_a = 11.4^\circ$, $Z_{op} = 45.44 \Omega$, $\Theta_{op} = 22.5^\circ$ $w_{Z_a} = 0.35$ mm, $\ell_{\Theta_a} = 7.03$ mm, $w_{Z_{op}} = 1.73$ mm, $\ell_{\Theta_{op}} = 13.29$ mm |
| $Z_t = 110 \Omega$, $\Theta_t = 12.16^\circ$, $Z_{op1} = 42.83 \Omega$, $\Theta_{op1} = 45^\circ$, $Z_{op2} = 24.73 \Omega$, $\Theta_{op2} = 30^\circ$ for Z_{b1} $w_{Z_t} = 0.34$ mm, $\ell_{\Theta_t} = 7.51$ mm, $w_{Z_{op1}} = 1.89$ mm, $\ell_{\Theta_{op1}} = 26.51$ mm, $w_{Z_{op2}} = 3.9$ mm, $\ell_{\Theta_{op2}} = 17.27$ mm. |
| $Z_t = 110 \Omega$, $\Theta_t = 17.13^\circ$, $Z_{op1} = 37.63 \Omega$, $\Theta_{op1} = 30^\circ$, $Z_{op2} = 65.18 \Omega$, $\Theta_{op2} = 45^\circ$ for Z_{b2} $w_{Z_t} = 0.34$ mm, $\ell_{\Theta_t} = 10.58$ mm, $w_{Z_{op1}} = 2.26$ mm, $\ell_{\Theta_{op1}} = 17.57$ mm, $w_{Z_{op2}} = 0.98$ mm, $\ell_{\Theta_{op2}} = 27.1$ mm. |

differently as 22.5° , 30° , and 45° long at f_0 , respectively. So, different open stubs for the S_{21} -path are required.

IV. DESIGNS AND MEASUREMENTS

Considering the design guidelines and power flow mechanism, three examples for $k = 1$ (0 dB), $k = 2$ (6 dB) and $k = 5.62$ (15 dB) will be designed for HSBHs at the design frequency of $f_0 = 1$ GHz. Two for $k = 1$ and $k = 2$ will be measured and the layout of one for $k = 5.62$ will be illustrated.

A. Prototype I for $k = 1$ (0 dB)

The prototype I for $k = 1$ was designed and fabricated on a substrate (RT/duriod 5870, $\epsilon_r = 2.33$, $H = 20$ mil). If $Z_{b1} = 28.28 \Omega$ is selected, $Z_{b2} = 40 \Omega$ is calculated in (10a). Choosing arbitrary values of $Z_{op} = 45.44 \Omega$ and $\Theta_{op} = 22.5^\circ$ gives $Z_a = 108.6 \Omega$ and $\Theta_a = 11.4^\circ$ in (10). Then, the TLs for Z_{b1} and Z_{b2} should be replaced with the $ML_{s2}T$ -types for HSBHs.

For $Z_{b1} = 28.28 \Omega$, since the characteristic impedance is low enough, the inductance values of L_s for the $ML_{s2}T$ -types are not necessary, leading to $N = 2$ with $\Theta_r = 0^\circ$. If it is assumed that the highest feasible value for Z_t is 110Ω , the electrical length of Θ_t should be 12.16° by the formula in (14a). To allocate the TZ at $3f_0$ using the open stub with Z_{op1} and Θ_{op1} in Fig. 5(b), the electrical length of Θ_{op1} should be 30° referring to (15). The corresponding characteristic impedance of Z_{op1} can be calculated in (14b). Another T -type can be designed to have a TZ at $2f_0$, or, $\Theta_{op2} = 45^\circ$. From the two open stubs of the T -types, two TZs at $2f_0$ and $3f_0$ can be obtained successfully. To have the third TZ at $4f_0$, the open stub of the L -section should be 22.5° long. For the TL with $Z_{b2} = 40 \Omega$, the $ML_{s2}T$ -type can be designed similarly. The design and fabrication parameters are listed in Table II where w_{Z_a} , $w_{Z_{op}}$, \dots , are the corresponding widths for the characteristic impedances of Z_a , Z_{op} , \dots , respectively, while ℓ_{Θ_a} , $\ell_{\Theta_{op}}$, \dots , are the lengths for Θ_a , Θ_{op} , \dots , respectively.

The fabricated prototype I is displayed in Fig. 8, while the measured results are compared with the predicted ones

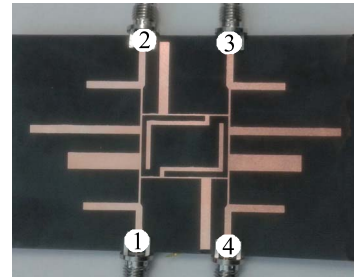


Fig. 8. Fabricated HSBH for $k = 1$.

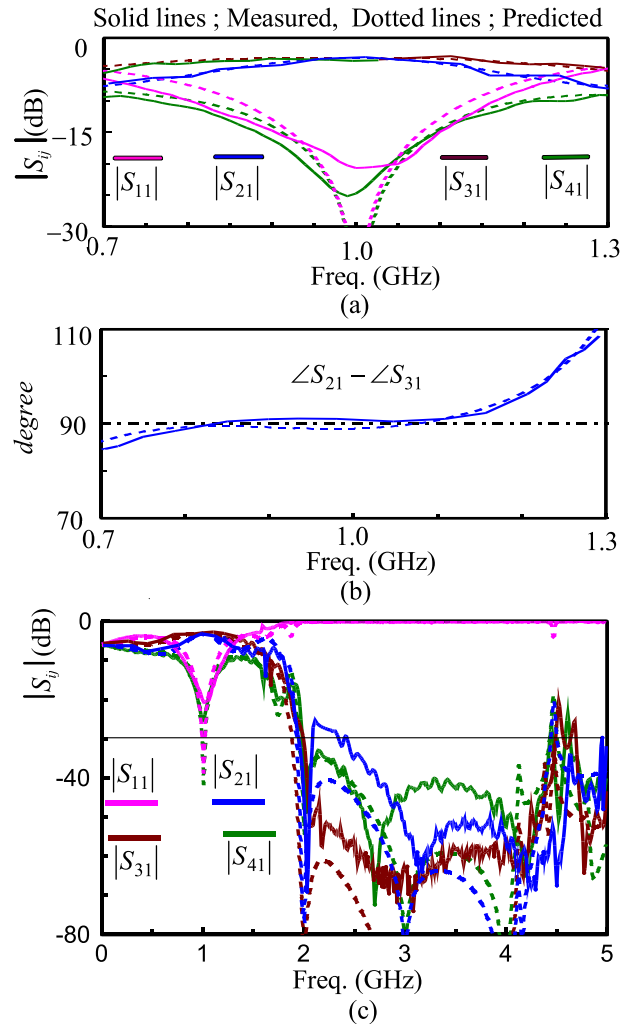


Fig. 9. Predicted and measured frequency responses for $k = 1$. (a) Scattering parameters around $f_0 = 1$ GHz. (b) Phase difference between S_{21} and S_{31} around $f_0 = 1$ GHz. (c) Scattering parameters for 1–5 GHz.

in Fig. 9 where the frequency responses of scattering parameters and the phase difference between S_{21} and S_{31} are plotted around $f_0 = 1$ GHz in Fig. 9(a) and (b), respectively, while those of scattering parameters from 0 to 5 GHz in Fig. 9(c).

The measured matching at port ① $|S_{11}|$, the power divisions of $|S_{21}|$ and $|S_{31}|$ and the isolation $|S_{41}|$ at 1 GHz is -20.95 , -3.05 , -3.17 , and -24.87 dB in Fig. 9(a) and the phase difference between S_{21} and S_{31} at f_0 is 88.5° in Fig. 9(b). The measured scattering values of $|S_{21}|$ at 2.0, 3.0, and 4.0 GHz

TABLE III
DESIGN AND FABRICATION PARAMETERS FOR $k = 2$

| |
|---|
| $Z_{b1} = 30 \Omega, Z_{b2} = 67.08 \Omega$ |
| $Z_a = 109.22 \Omega$ and $\Theta_a = 13.06^\circ$ $(Z_{op}, \Theta_{op}) = (31.89 \Omega, 22.5^\circ)$ at port ① $(Z_{op}, \Theta_{op}) = (55.94 \Omega, 36^\circ)$ at ports ②, ③ and ④ $w_{Z_a} = 0.54 \text{ mm}, \ell_{\Theta_a} = 8.1 \text{ mm}, w_{Z_{op}} = 4.37 \text{ mm}, \ell_{\Theta_{op}} = 13.08 \text{ mm}$ at port ① for $\Theta_{op} = 22.5^\circ$. $w_{Z_{op}} = 1.96 \text{ mm}, \ell_{\Theta_{op}} = 21.47 \text{ mm}$ at port ②, ③ and ④ for $\Theta_{op} = 36^\circ$. |
| $L_s = \Theta_r = 0, N = 2, Z_t = 94.39 \Omega, \Theta_t = 15^\circ, Z_{op1} = 27.25 \Omega, \Theta_{op1} = 30^\circ, Z_{op2} = 47.19 \Omega, \Theta_{op2} = 45^\circ$ for Z_{b1} . $w_{Z_t} = 0.75 \text{ mm}, \ell_{\Theta_t} = 9.19 \text{ mm}, w_{Z_{op1}} = 5.36 \text{ mm}, \ell_{\Theta_{op1}} = 17.33 \text{ mm}, w_{Z_{op2}} = 2.54 \text{ mm}, \ell_{\Theta_{op2}} = 26.62 \text{ mm}$ |
| $N = 1, Z_r = 90 \Omega, \Theta_r = 3^\circ, L_s = 5.6 \text{ nH}, Z_t = 90 \Omega, \Theta_t = 30.85^\circ, \Theta_{t2} = 0^\circ, Z_{op1} = 42.08 \Omega, \Theta_{op1} = 22.5^\circ$ for Z_{b2} . $w_{Z_r} = 0.83 \text{ mm}, \ell_{\Theta_r} = 1.83 \text{ mm}, w_{Z_t} = 0.83 \text{ mm}, \ell_{\Theta_t} = 18.85 \text{ mm}, w_{Z_{op1}} = 3.21 \text{ mm}, \ell_{\Theta_{op1}} = 13.21 \text{ mm}$ |

are -51.8 , -52.3 , and -57.3 dB, respectively, and can be suppressed by more than 50 dB, even though the designed TZ frequencies are shifted slightly.

B. Prototype II for $k = 2$ (6 dB)

The prototype II was designed and fabricated on a substrate (RT/duriod 5870, $\epsilon_r = 2.33$, $H = 31$ mil). One case for $Z_{b1} = 30 \Omega$ and $Z_{b2} = 67.08 \Omega$ in Table I will be designed for the HSBH.

Since the characteristic impedance of $Z_{b1} = 30 \Omega$ is sufficiently low, the $ML_{s2}T$ -types in Fig. 5(b) can be designed similarly to the case for $k = 1$ with $N = 2$ and $L_s = \Theta_r = 0$. For $Z_{b2} = 67.08 \Omega$, the characteristic impedance is relatively high and if the TLs are reduced using the $ML_{s2}T$ -type without L_s like the cases in Table II, the characteristic impedances of TLs should be too high to fabricate. Therefore L_s cannot be zero.

Since the 0603-sized chip inductors are $0.8+0.15/-0.10$ mm wide, the connected TL widths should be around 0.8 mm. Thus, the highest characteristic impedances of the TLs were determined as 100Ω whose width is 0.83 mm on the substrate. With arbitrarily chosen values of $Z_r = 90 \Omega$, $\Theta_r = 3^\circ$ and $L_s = 5.6$ nH and fixing at $Z_t = 90 \Omega$, the electrical length of $\Theta_{t1} = \Theta_t$, $\Theta_{t2} = 0$ can be calculated as $\Theta_t = 30.85^\circ$ based on (14a). To allocate a TZ at $4f_0$, Θ_{op1} should be 22.5° , resulting in the calculated value of $Z_{op1} = 42.08 \Omega$ from (14b). Only one open stub with $\Theta_{op1} = 22.5^\circ$ is possible from the $ML_{s2}T$ -type, and therefore additional TZs should be obtained by designing $\Theta_{op} = 22.5^\circ$ of the L -section at port ① and $\Theta_{op} = 36^\circ$ of the L -sections at ports ②, ③, and ④, differently. The electrical lengths of Θ_{op} can be adjusted under the same values of $Y_{op} \tan \Theta_{op}$, where $Y_{op} = Z_{op}^{-1}$. The design and fabrication parameters are listed in Table III where the L -sections with $Z_a = 109.22 \Omega$ and $\Theta_a = 13.06^\circ$ in Table I are used.

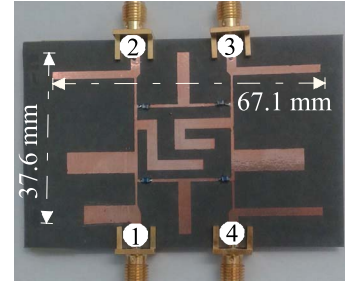


Fig. 10. Fabricated HSBH for $k = 2$ (6 dB).

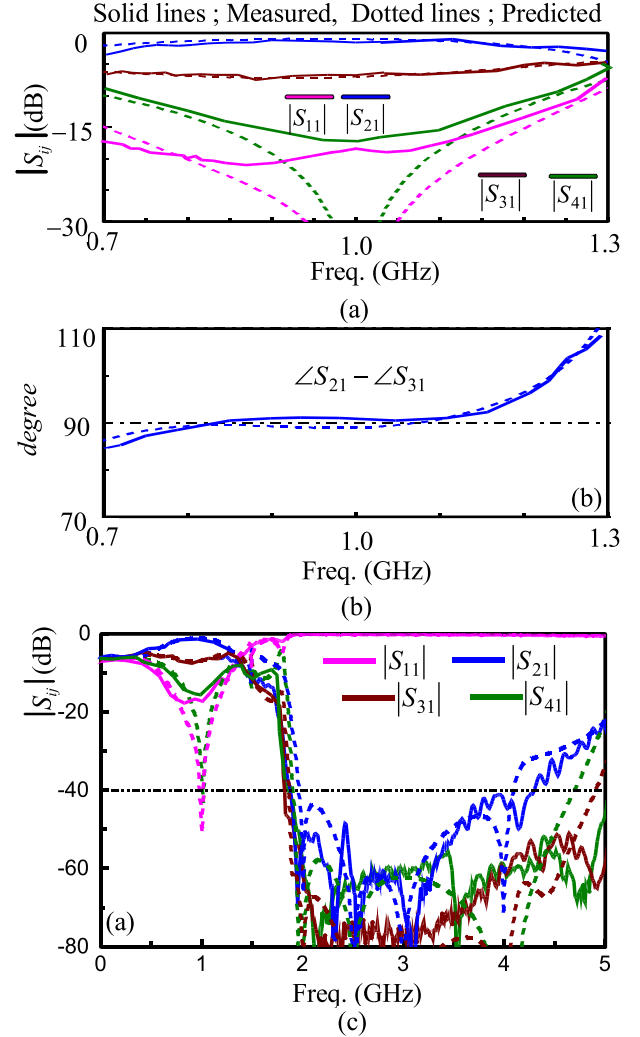


Fig. 11. Predicted and measured frequency responses for $k = 2$. (a) Scattering parameters around $f_0 = 1$ GHz. (b) Phase difference between S_{21} and S_{31} around $f_0 = 1$ GHz. (c) Scattering parameters for 1–5 GHz.

The fabricated prototype II is displayed in Fig. 10, and the measured frequency responses are compared with the predicted ones in Fig. 11 where the frequency responses of the scattering parameters and the phase difference between S_{21} and S_{31} is plotted around $f_0 = 1$ GHz in Fig. 11 (a) and (b), respectively, while those for the scattering parameters from 0 to 5 GHz in Fig. 11(c). The measured scattering parameters of $|S_{11}|$, $|S_{21}|$, $|S_{31}|$, and $|S_{41}|$ at 1 GHz are -17.87 , -1.03 , -6.91 , and

TABLE IV
DESIGN AND FABRICATION PARAMETERS FOR $k = 5.62$

| |
|--|
| $Z_{b1} = 28.28 \Omega, Z_{b2} = 161.53 \Omega$ |
| $Z_a = 90.35 \Omega, \theta_a = 16.77^\circ$ |
| $(Z_{op}, \theta_{op}) = (26.5 \Omega, 22.5^\circ)$ at port ① |
| $(Z_{op}, \theta_{op}) = (46.5 \Omega, 36^\circ)$ at ports ②, ③ and ④ |
| $w_{Z_a} = 0.53 \text{ mm}, \ell_{\theta_a} = 10.26 \text{ mm}, w_{Z_{op}} = 3.58 \text{ mm},$ |
| $\ell_{\theta_{op}} = 12.99 \text{ mm}$ at port ① for $\theta_{op} = 22.5^\circ$. $w_{Z_{op}} = 1.67$ |
| $\text{mm}, \ell_{\theta_{op}} = 21.29 \text{ mm}$ at port ②, ③ and ④ for $\theta_{op} = 36^\circ$. |
| $L_s = \theta_r = 0$ with $N = 2, Z_t = 100 \Omega, \theta_t = 13.36^\circ, Z_{op1} =$ |
| $25.1 \Omega, \theta_{op1} = 30^\circ, Z_{op2} = 43.47 \Omega, \theta_{op2} = 45^\circ$ for Z_{b1} . |
| $w_{Z_t} = 0.42 \text{ mm}, \ell_{\theta_t} = 8.21 \text{ mm}, w_{Z_{op1}} = 3.83 \text{ mm},$ |
| $\ell_{\theta_{op1}} = 17.28 \text{ mm}, w_{Z_{op2}} = 1.85 \text{ mm}, \ell_{\theta_{op2}} = 26.53 \text{ mm}.$ |
| $Z_r = 90 \Omega, \theta_r = 2^\circ, L_s = 22 \text{ nH}, Z_t = 100 \Omega, \theta_t = 12.34^\circ$ |
| $\theta_{t2} = 0^\circ, Z_{op1} = 101.8 \Omega, \theta_{op1} = 22.5^\circ$ for Z_{b2} |
| $w_{Z_r} = 0.53 \text{ mm}, \ell_{\theta_r} = 1.22 \text{ mm}, w_{Z_t} = 0.42 \text{ mm},$ |
| $\ell_{\theta_t} = 7.58 \text{ mm}, w_{Z_{op1}} = 0.41 \text{ mm}, \ell_{\theta_{op1}} = 13.84 \text{ mm}.$ |

−16.87 dB, respectively, resulting in the power-division ratio of 5.87 dB. The measured phase difference between S_{21} and S_{31} at 1 GHz is 90.8° in Fig. 11(b). The measured harmonic suppressions for $|S_{21}|$, $|S_{31}|$, and $|S_{41}|$ can be achieved from $2f_0$ to $4f_0$ by more than 40 dB as can be shown in Fig. 11(c).

C. Prototype III for $k = 5.62$ (15 dB)

For $k = 5.62$, the conventional characteristic impedances for two 90° TLs in [1] are 49.23 and 281.18 Ω which is, in any case, impossible to fabricate in a microstrip format. For HSBHs, the two 281.18- Ω TLs should be reduced, leading to extremely high values of the characteristic impedances. However, if using the suggested BH and $ML_{s2}T$ -types, the conventional fabrication problem can be solved.

If Z_{b1} is chosen as 28.28 Ω , the Z_{b2} can be calculated as $Z_{b2} = 161.53 \Omega$. Similarly to the case for $k = 2$, the design and fabrication parameters on the same substrate for $k = 1$ are listed in Table IV based on which the layout is illustrated in Fig. 12 where the gaps are for soldering off-the-self chip inductors (0402 size).

The simulated frequency responses around $f_0 = 1$ GHz are in Fig. 13(a) and (b), while those from 0 to $5f_0$ in Fig. 13(c). The scattering parameters for S_{12} and S_{13} are −0.13 and −15.13 dB at f_0 , respectively, leading to the power division ratio of 15 dB. Perfect matching, perfect isolation and perfect phase responses are achieved at f_0 , and the scattering parameters of $|S_{21}|$ and $|S_{31}|$ can be suppressed by more than 40 dB from $2f_0$ to $4f_0$. The 15-dB return loss bandwidth for $|S_{11}|$ is more than 100% (0.36–1.37 f_0).

From the two types of measurements and the layout in Fig. 12, one can understand that as far as the characteristic impedance of Z_t for Z_{b2} is feasible and the values for Z_{b1} are not less than 28.28 Ω , any HSBH can be fabricated with a microstrip format. However the parasitic radiation from the stubs sets a limitation on the feasible power-division ratios at the higher frequencies such as $4f_0$.

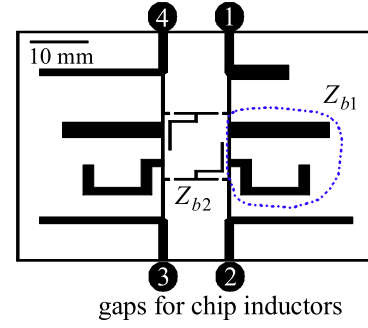


Fig. 12. Layout of the HSBH for $k = 5.62$.

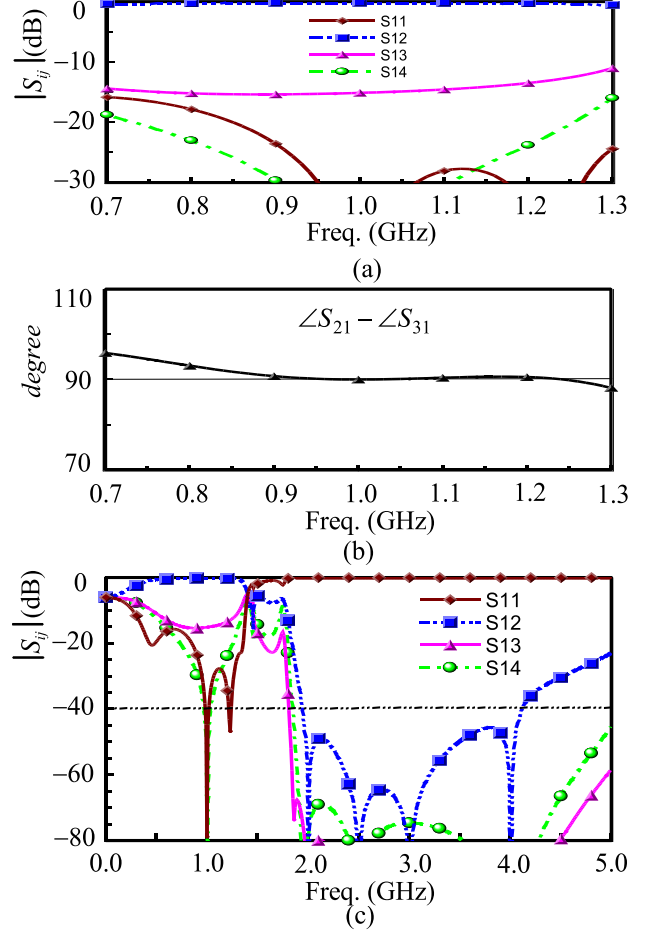


Fig. 13. (a) Simulated frequency responses of $|S_{11}|$, $|S_{21}|$, $|S_{31}|$, and $|S_{41}|$ around $f_0 = 1$ GHz for $k = 5.62$ (b) Phase difference between S_{21} and S_{31} . (c) Frequency responses from 0 to $5f_0$.

D. Comparisons With Conventional Works

The prototype II for $k = 2$ (6 dB) is compared with the previous works [3]–[15] in terms of arbitrary power-division ratios (Apsds), achievable highest power-division ratio (Highest k), Size (λ_g^2), selectivity for more than three TZs (selectivity), the suppression of the $2f_0$ signal ($2f_0$), 30 dB suppression bandwidths of S_{21} from $2f_0$ $\{(f_2 - f_1)/f_0\}$ where f_2 and f_1 are band-edge frequencies, 15-dB return loss bandwidths of $|S_{11}|$ around f_0 ($|S_{11}|$ BW) and design frequencies (f_0).

The comparisons data are collected in Table V where the possibility or impossibility are expressed as “o” and “x,” respectively. For the prototype II, the occupied physical size is 67.1 mm \times 37.6 mm in Fig. 10, leading to 0.17×0.30 (λ_g^2)

TABLE V
COMPARISONS WITH CONVENTIONAL WORKS

| Refs. | Apds. | Highest k (dB) | Size (λ_g^2) | Selectivity | $2f_0$ | $(f_2 - f_1)/f_0$ | $ S_{11} BW$ (%) | f_0 (GHz) |
|--------------------------|-------|------------------|----------------------------|-------------|--------|-------------------|------------------|-------------|
| This work (prototype II) | o | 15 dB | 0.17 x 0.30 | o | o | 262% | $\approx 50\%$ | 1 |
| [3] | o | 8.41 dB | 0.75 x 0.25 | x | x | 0 % | 57 % | 3 |
| [4] | x | 0 dB | 0.11 x 0.12 | x | x | a few % | $\approx 7\%$ | 0.83 |
| [5] | x | 0 dB | 0.22 x 0.22 | x | x | 220 % | 14% | 2.4 |
| [6] | x | 0 dB | 0.09 x 0.14 | x | x | 0 % | 22 % | 0.9 |
| [7] | x | 0 dB | 0.13 x 0.13 | x | o | a few % | 10 % | 2 |
| [8] | x | 0 dB | $\approx 0.14 \times 0.14$ | x | x | a few % | $< 10\%$ | 0.9 |
| [9] | x | 0 dB | 0.23 x 0.29 | x | o | 0 % | ≈ 76.6 | 1.1 |
| [10] | x | 0 dB | $\approx 0.49 \times 0.49$ | x | x | 0 % | 23.7 % | 2.6 |
| [11] | x | 0 dB | $\approx 0.15 \times 0.15$ | x | x | 0 % | $\approx 50\%$ | 2.45 |
| [12] | x | 0 dB | $\approx 0.12 \times 0.15$ | x | x | a few % | $\approx 16.7\%$ | 0.9 |
| [13] | x | 0 dB | 0.19x 0.19 | x | o | 0 % | $\approx 18\%$ | 1 |
| [14] | o | 9.54 dB | 0.5 x 0.47 | x | o | a few % | 30.5 % | 3 |
| [15] | x | 0 dB | 0.05 x 0.46 | x | x | a few % | $\approx 27.8\%$ | 0.9 |

Apds : Arbitrary power division, Highest k : Highest feasible value of k , o or x : Possible or impossible, Size (λ_g^2) : Required size where λ_g is a wavelength at f_0 , Selectivity : Selective harmonic suppression, f_0 : Design frequency, $2f_0$: Second harmonic suppression, $(f_2 - f_1)/f_0$: Harmonic suppression bandwidths from $2f_0$, $|S_{11}|BW$ (%) : 15 dB return loss bandwidths around f_0 .

which can be obtained by converting physical lengths into the electrical wavelengths based on the substrate and f_0 .

More than three TZs can be achieved by designing the open stubs differently, and the wideband harmonic suppression from $2f_0$ can be achieved as well. The band edge frequencies of f_2 and f_1 for 30 dB suppression are 4.53 and 1.91 f_0 , resulting in the harmonic suppression BW of 262 %. The power-division ratio of the prototype II is only 6 dB but the highest achievable value for k can be 15 dB based on the design parameters in Table IV, the layout in Fig. 12 and simulated frequency responses in Fig. 13.

On the other hands, only [3] and [14] can be possible for the arbitrary power divisions, and the achievable highest values of k are 8.41 and 9.54 dB, respectively. The $2f_0$ signal can be suppressed somehow in [5], [7], and [11] but no selective TZ is possible. The BH in [3] consists of four 90° TLs and four additional 90° TLs, leading to the occupied area of $0.75 \times 0.25 \lambda_g^2$. The one in [14] uses L_T - and Π -types [16], [17] and the occupied area are $0.5 \times 0.49 \lambda_g^2$. In the similar way, other BHs' areas can be estimated as compared in Table V.

From the comparison data, one can understand that no previous work can provide such highest power-division ratios for HSBHs with compact size, no previous work is possible for more than three selective TZs, no previous work can provide such high performance with more than 30 dB suppression including $2f_0$ and no previous work can provide such wideband harmonic suppression from $2f_0$ to $4f_0$.

V. CONCLUSION

In this paper, a BH topology was presented, consisting of four TLs and four identical L -sections with each a TL and an open stub. The suggested BH topology can provide as

low characteristic impedances of the TLs as possible, longer electrical paths for the scattering parameters and additional TZs by which high performance with more than 30 dB harmonic suppression, wideband ($2-4f_0$) and selective harmonic suppression can be achieved. The size of HSBHs can be more compact than any other conventional work for arbitrary power-division ratios, and the suggested HSBHs can be applied for highest power-division ratios, as well.

REFERENCES

- [1] H.-R. Ahn and I. Wolff, "Asymmetric four-port and branch-line hybrids," *IEEE Trans. Microw. Theory Techn.*, vol. 48, no. 9, pp. 1585–1588, Sep. 2000.
- [2] H.-R. Ahn and S. Nam, "Compact microstrip 3-dB coupled-line ring and branch-line hybrids with new symmetric equivalent circuits," *IEEE Trans. Microw. Theory Techn.*, vol. 61, no. 3, pp. 1067–1078, Mar. 2013.
- [3] K. A. Alshamaileh, V. K. Devabhaktuni, and N. I. Dib, "Impedance-varying broadband 90° branch-line coupler with arbitrary coupling levels and higher order harmonic suppression," *IEEE Trans. Compon., Packag., Manuf. Technol.*, vol. 5, no. 10, pp. 1507–1515, Oct. 2015.
- [4] K.-Y. Tsai, H.-S. Yang, J.-H. Chen, and Y.-J. E. Chen, "A miniaturized 3 dB branch-line hybrid coupler with harmonics suppression," *IEEE Microw. Wireless Compon. Lett.*, vol. 21, no. 10, pp. 537–539, Oct. 2011.
- [5] P. Mondal and A. Chakrabarty, "Design of miniaturised branch-line and rat-race hybrid couplers with harmonics suppression," *IET Microw., Antennas Propag.*, vol. 3, no. 1, pp. 109–116, Feb. 2009.
- [6] J. Kim and J.-G. Yook, "A miniaturized 3 dB 90° hybrid coupler using coupled-line section with spurious rejection," *IEEE Microw. Wireless Compon. Lett.*, vol. 24, no. 11, pp. 766–768, Nov. 2014.
- [7] J. Wang, B.-Z. Wang, Y.-X. Guo, L. C. Ong, and S. Xiao, "A compact slow-wave microstrip branch-line coupler with high performance," *IEEE Microw. Wireless Compon. Lett.*, vol. 17, no. 7, pp. 501–503, Jul. 2007.
- [8] K. V. P. Kumar and S. S. Karthikeyan, "Miniaturised quadrature hybrid coupler using modified T-shaped transmission line for wide-range harmonic suppression," *IET Microw., Antennas Propag.*, vol. 10, no. 14, pp. 1522–1527, Nov. 2016.

- [9] V. K. Velidi, B. Patel, and S. Sanya, "Harmonic suppressed compact wideband branch-line coupler using unequal length open-stub units," *Int. J. RF Microw. Comput.-Aided Eng.*, vol. 21, no. 1, pp. 115–119, Jan. 2011.
- [10] M. Nosrati, M. Daneshmand, and B. S. Virdee, "Novel compact dual-narrow/wideband branch-line couplers using T-Shaped stepped-impedance-stub lines," *Int. J. RF Microw. Comput.-Aided Eng.*, vol. 21, no. 6, pp. 642–649, Nov. 2011.
- [11] Y. S. Wong, S. Y. Zheng, and W. S. Chan, "A wideband coupler with wide suppression band using coupled stub," in *Proc. Asia-Pacific Microw. Conf.*, Dec. 2011, pp. 1058–1061.
- [12] C.-W. Wang, T.-G. Ma, and C.-F. Yang, "Miniaturized branch-line coupler with harmonic suppression for RFID applications using artificial transmission lines," in *IEEE MTT-S Int. Microw. Symp. Dig.*, Jun. 2007, pp. 29–32.
- [13] V. K. Velidi, A. V. G. Subramanyam, V. S. Kumar, Y. Mehta, and S. Sanyal, "Compact harmonic suppression branch-line coupler using signal-interference technique," in *Proc. Asia-Pacific Microw. Conf. (APMC)*, Dec. 2016, pp. 1–4.
- [14] Z. Qamar, S. Y. Zheng, W. S. Chan, and D. Ho, "Coupling coefficient reconfigurable wideband branch-line coupler topology with harmonic suppression," *IEEE Trans. Microw. Theory Techn.*, vol. 66, no. 4, pp. 1912–1920, Apr. 2018.
- [15] R. K. Barik, R. Rajender, and S. S. Karthikeyan, "A miniaturized wideband three-section branch-line hybrid with harmonic suppression using coupled line and open-ended stubs," *IEEE Microw. Wireless Compon. Lett.*, vol. 27, no. 12, pp. 1059–1061, Dec. 2017.
- [16] H.-R. Ahn and S. Nam, "Wideband microstrip coupled-line ring hybrids for high power-division ratios," *IEEE Trans. Microw. Theory Techn.*, vol. 61, no. 5, pp. 1768–1780, May 2013.
- [17] H.-R. Ahn and S. Nam, "New design formulas for impedance-transforming 3-dB Marchand baluns," *IEEE Trans. Microw. Theory Techn.*, vol. 59, no. 11, pp. 2816–2823, Nov. 2011.
- [18] J. Reed and G. J. Wheeler, "A method of analysis of symmetrical four-port networks," *IRE Trans. Microw. Theory Techn.*, vol. MTT-4, no. 4, pp. 246–252, Oct. 1956.



Hee-Ran Ahn (S'90–M'95–SM'99) received the B.S., M.S., and Ph.D. degrees in electronic engineering from Sogang University, Seoul, South Korea.

From 1996 to 2002, she was with the Department of Electrical Engineering, Duisburg-Essen University, Duisburg, Germany, where she was involved with the habilitation dealing with asymmetric passive components in microwave-integrated circuits. From 2003 to 2005, she was with the Department of Electrical Engineering and Computer Science, Korea Advanced Institute of Science and Technology, Daejeon, South Korea. From 2005 to 2009, she was with the Department of Electronics and Electrical Engineering, Pohang University of Science and Technology, Pohang, South Korea. From 2009 to 2010, she was with the Department of Electrical Engineering, University of California at Los Angeles, Los Angeles, CA, USA. From 2011 to 2014, she was with the School of Electrical Engineering and Computer Science, Seoul National University, Seoul. Since 2015, she has been as a Visiting Scholar with the School of Electrical and Computer Engineering, Georgia Institute of Technology, Atlanta, GA, USA. She authored *Asymmetric Passive Component in Microwave Integrated Circuits* (Wiley, 2006). Her current research interests include high-frequency and microwave circuit designs and biomedical applications using microwave theory and techniques.



Manos M. Tentzeris (M'98–SM'03–F'10) received the diploma degree (*magna cum laude*) in electrical and computer engineering from the National Technical University of Athens, Athens, Greece, and the M.S. and Ph.D. degrees in electrical engineering and computer science from the University of Michigan, Ann Arbor, MI, USA.

He is currently a Ken Byers Professor of Flexible Electronics with the School of Electrical and Computer Engineering, Georgia Institute of Technology, Atlanta, GA, USA. He was a Visiting Professor with the Technical University of Munich, Germany, for the summer of 2002, a Visiting Professor with GTRI-Ireland in Athlone, Ireland, for the summer of 2009 and a Visiting Professor with LAAS-CNRS in Toulouse, France, for the summer of 2010. He has authored over 700 papers in refereed journals and conference proceedings, 5 books, and 25 book chapters. He has helped develop academic programs in 3-D/inkjet-printed RF electronics and modules, flexible electronics, origami and morphing electromagnetics, highly integrated/multilayer packaging for RF and wireless applications using ceramic and organic flexible materials, paper-based RFIDs and sensors, wireless sensors and biosensors, wearable electronics, "Green" electronics, energy harvesting and wireless power transfer, nanotechnology applications in RF, microwave MEMS, SOP-integrated (UWB, multiband, millimeter wave, and conformal) antennas and heads the ATHENA research group (20 researchers).

Dr. Tentzeris is a member of URSI-Commission D, a member of the IEEE MTT-15 Committee, an Associate Member of EuMA, a Fellow of the Electromagnetic Academy, and a member of the Technical Chamber of Greece. He was a recipient or co-recipient of the 2015 IET Microwaves, Antennas and Propagation Premium Award, the 2014 Georgia Institute of Technology Electrical and Computer Engineering Distinguished Faculty Achievement Award, the 2014 IEEE RFID-TA Best Student Paper Award, the 2013 IET Microwaves, Antennas and Propagation Premium Award, the 2012 FiDiPro Award in Finland, the iCMG Architecture Award of Excellence, the 2010 IEEE Antennas and Propagation Society Piergiorgio L. E. Uslenghi Letters Prize Paper Award, the 2011 International Workshop on Structural Health Monitoring Best Student Paper Award, the 2010 Georgia Institute of Technology Senior Faculty Outstanding Undergraduate Research Mentor Award, the 2009 IEEE TRANSACTIONS ON COMPONENTS AND PACKAGING TECHNOLOGIES Best Paper Award, the 2009 E. T. S. Walton Award from the Irish Science Foundation, the 2007 IEEE APS Symposium Best Student Paper Award, the 2007 IEEE MTT-S IMS Third Best Student Paper Award, the 2007 ISAP 2007 Poster Presentation Award, the 2006 IEEE MTT Outstanding Young Engineer Award, the 2006 Asia-Pacific Microwave Conference Award, the 2004 IEEE TRANSACTIONS ON ADVANCED PACKAGING Commendable Paper Award, the 2003 NASA Godfrey "Art" Anzic Collaborative Distinguished Publication Award, the 2003 IBC International Educator of the Year Award, the 2003 IEEE CPMT Outstanding Young Engineer Award, the 2002 International Conference on Microwave and Millimeter-Wave Technology Best Paper Award (Beijing, China), the 2002 Georgia Institute of Technology-Electrical and Computer Engineering Outstanding Junior Faculty Award, the 2001 ACES Conference Best Paper Award and the 2000 NSF CAREER Award, and the 1997 Best Paper Award of the International Hybrid Microelectronics and Packaging Society. He served as the Head of the GT-ECE Electromagnetics Technical Interest Group, as the Georgia Electronic Design Center Associate Director for RFID/Sensors Research, as the Georgia Institute of Technology NSF-Packaging Research Center Associate Director for RF Research, and the RF Alliance Leader. He was the TPC Chair for IEEE MTT-S IMS 2008 Symposium and the Chair of the 2005 IEEE CEM-TD Workshop and he is the Vice-Chair of the RF Technical Committee of the IEEE CPMT Society. He is the founder and the Chair of the RFID Technical Committee of the IEEE MTT-S and the Secretary/Treasurer of the IEEE C-RFID. He is an Associate Editor of the IEEE TRANSACTIONS ON MICROWAVE THEORY AND TECHNIQUES, the IEEE TRANSACTIONS ON ADVANCED PACKAGING, and the *International Journal on Antennas and Propagation*. He has given more than 100 invited talks to various universities and companies all over the world. He served as one of the IEEE MTT-S Distinguished Microwave Lecturers from 2010 to 2012 and one of the IEEE CRFID Distinguished Lecturers.